Pergamon

Journal of Structural Geology, Vol. 18, No. 5, pp. 625 to 642, 1996

0191-8141/96 $15.00+0.00

0191-8141(95)00125-5

Multiple crenulation cleavages as kinematic and incremental strain indicators

RACHEL BURKS

Department of Physics, Towson State University, Towson, MD 21204-7097, U.S.A.

and

SHARON MOSHER

Department of Geological Sciences, University of Texas at Austin, Austin, TX 78712, U.S.A.

(*Received* 12 *December* 1994, *accepted in revised form* 30 *September* 1995)

Abstract—Well-foliated metasedimentary rocks within strike-slip shear zones from the Narragansett Basin of Rhode Island are deformed by superposed crenulation cleavages. Overprinting relationships between cleavage generations is consistently clockwise or anti-clockwise in sinistral and dextral shear zones, respectively, indicating that the cleavages formed during progressive non-coaxial deformation. These shear zones have a nearly ideal geometry relative to the pre-existing foliation that allowed sequential formation and rotation of each crenulation generation.

In this paper, we explore the formation of these superposed crenulation cleavages and propose a method for measuring the incremental strains recorded by the cleavages. The effects of a variably oriented pre-existing foliation are considered and incorporated into the model. The superposed crenulation cleavages provide a new kinematic indicator for well-foliated rocks that records the deformation path and the associated incremental strains. Copyright © 1996 Elsevier Science Ltd

INTRODUCTION

In reconstructing the tectonic history of a region, structural geologists generally rely on structural styles, orientations and overprinting geometries, finite strain data, and kinematic indicators in shear zones. Only rarely do rocks record the deformation path or incremental strains that led to the final state. Fibrous veins and pressure shadows are among the few structures that both record the deformation path and allow the incremental strains to be measured (e.g. Durney & Ramsay 1973, Wickham 1973, Ramsay & Huber 1983, pp. 235–280). Although the deformation path is also recorded by layers that underwent first folding then boudinage (Ramsay 1967), the incremental strains are not measurable. In most other cases, the path must be deduced by comparing final and probable initial states.

In this paper, a new kinematic indicator, superposed crenulation cleavages, that tracks the deformation path within shear zones is discussed, and a three-dimensional geometric technique is developed that quantifies the incremental strains resulting from progressive simple shear. Extremely well-developed superposed crenulation cleavages are found in Late Paleozoic, strike- and oblique-slip shear zones in the southern Narragansett Basin of Rhode Island (Berryhill 1984, Burks 1984, 1985, Mosher & Berryhill 1991). The cleavages formed during progressive non-coaxial deformation of a pre-existing, penetrative, planar, metamorphic foliation and record discrete increments of strain.

Regional setting

The Narragansett Basin of Rhode Island and Massachusetts is a Pennsylvanian-age composite graben system that records a complex history of Alleghanian deformation and Barrovian metamorphism ranging from lower greenschist to upper amphibolite facies (Skehan & Murray 1979, Mosher 1983, Snoke & Mosher 1989). The sedimentary sequence consists of laterally discontinuous, interbedded sandstone, shale, conglomerates and minor coal. Early syn-metamorphic deformation of the basin-fill produced multiple generations of generally isoclinal folds with associated axial-planar foliations. These structures occur throughout the southern portion of the basin. The most pronounced structure at most outcrops is a relatively planar, horizontal to gently dipping, penetrative foliation (S_1). This foliation is locally deformed by a number of nearly vertical ductile shear zones oriented NNE, NE and ENE that divide the southern portion of the basin into large blocks (Fig. 1). The rocks within these blocks show only the early deformation, whereas the intensely deformed rocks within shear zones contain multiple generations of later structures. The most intense deformation is concentrated in a N30°E-trending zone, the Beaverhead shear zone, that cuts across the central portion of the southern basin (Burks 1985). This zone consists of a series of smaller interconnected NNE, NE and ENE shear zones. The shear zones are parallel to faults that bound intrabasinal horsts and graben, some of which

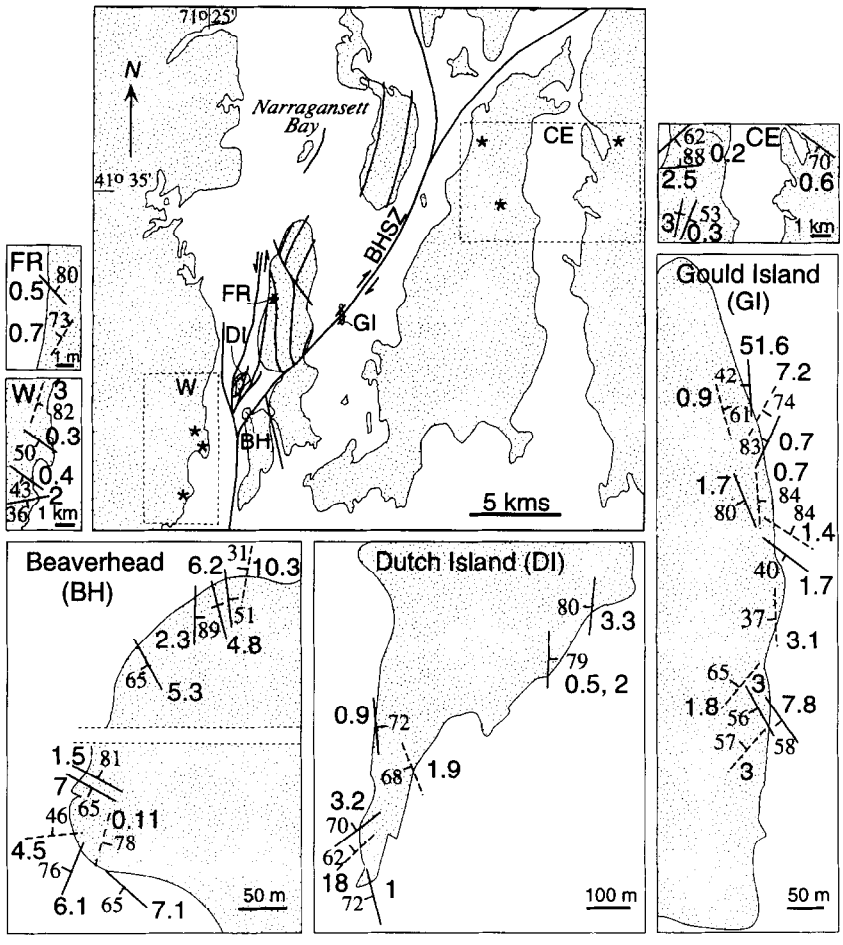

Fig. 1. Regional map of Narragansett Bay showing major shear zones (after Cogswell & Mosher 1994). NE-trending zones are dextral; N-trending zones are sinistral. (BHSZ—Beaverhead shear zone; other initials correspond to smaller maps for individual localities listed in Table 1.) Small maps show orientations of calculated shear planes and incremental shear strains. Dashed lines are dextral; solid lines are sinistral. FR—Fowler Rocks; shear zones location shown by ⋆ on regional map; W—western coast, CE—central and eastern areas; location of maps shown by dashed box on regional map and specific shear zones locations shown by ⋆. GI—Gould Island; BH—Beaverhead; DI—Dutch Island.

were active during sedimentation (Henderson & Mosher 1983, Mosher 1983). Thus, the shear zones affecting the metasedimentary rocks may have formed above reactivated basement faults.

Shear zones

Most shear zones in the Narragansett Basin deform very fine-grained phyllites or graphitic schists that are well-bedded and have a well-developed pre-existing foliation at a high angle to the shear plane. Thus, the resultant structures are folds, crenulation cleavages, tension gashes, extension fractures and boudins. Zones with relatively small displacements contain en echelon folds, boudins or one generation of shear-related folds, whereas major zones contain multiple generations of superposed, non-coaxial folds or crenulation cleavages (Mosher 1983, Mosher & Berryhill 1991). A few moderately dipping zones also contain sheath folds. Zones range in width from centimeters to more than 20 m. Lengths and widths of some zones are indeterminate, because most crop out along the coast of numerous islands within Narragansett Bay (Fig. 1). Although the boundaries of some shear zones are not exposed, the zones are identified by the deformation intensity and presence of kinematic indicators showing a consistent sense of movement.

Most NNE-trending zones are vertical and record sinistral strike-slip motion, whereas NE-trending zones have steep to moderate dips and show dextral motion. Where zones meet, NNE-trending zones are deflected into or overprinted by NE-trending zones (Mosher & Berryhill 1991). Some of the NNE- and NE-trending zones are cut by parallel brittle faults that may or may not be related to the strike-slip motion. Sinistral zones are generally the widest, and many shear zone boundaries are not exposed. Between one and three generations of large-scale, NNE- to NE-trending folds and up to four generations of crenulation cleavages are observed. The superposed non-coaxial fold and crenulation cleavage generations show a consistent clockwise younging. A major sinistral zone apparently lies in the west passage of Narragansett Bay with the main effects observed on Dutch Island (Fig. 1) (Mosher & Berryhill 1991, Cogswell & Mosher 1994). Splays off this zone affect rocks along the adjacent coastlines, and other less major zones affect rocks further east. Dextral zones are narrower, have observable boundaries, and show de-

monstrable offset and reorientation of previous structures. Shear-related structures include one generation of large-scale, N-trending folds, up to four generations of small-scale, N- to NE-trending folds, and up to four generations of crenulation cleavages. The superposed, non-coaxial fold and crenulation cleavage generations show a consistent anti-clockwise younging. Boudinage is common, and where shear zones have moderate dips, sheath folds are abundant. Six zones with significant displacement and numerous minor zones are found within the Beaverhead shear zone. The generally narrow, vertical ENE-trending zones post-date the NE-trending zones and are associated with brittle normal faults with a minor dextral component. Although these latter zones deflect the pre-existing structures, no new ductile structures are formed.

Shear zones formed late in the metamorphic history. Veins within shear zones are mainly quartz with some chlorite and white mica. No new metamorphic minerals have grown parallel to the crenulation cleavages or overgrow them. Generally more brittle structures are found in dextral zones, which, coupled with the narrower widths, suggests that deformation became more brittle with time (Mosher & Berryhill 1991). Waning temperatures, differences in strain rate or amount of displacement for a given zone width, and strain hardening could all explain the increase in brittle deformation. For a detailed description of shear zones and the kinematic indicators in one area (Dutch Island), see Mosher & Berryhill (1991).

SUPERPOSED CRENULATION CLEAVAGES

Within shear zones, several generations of crenulation cleavages are well developed and crenulate the pervasive S_1 foliation. Although some conjugate sets of crenulations are present, most cleavages are at angles of less than 30° to one another and show a consistent overprinting relationship across an entire outcrop (Fig. 2a). Where exposure is good, individual cleavage generations can be tracked for tens of meters. As many as four clockwise and four anti-clockwise younging cleavages have been documented (Berryhill 1984, Burks 1985, Mosher & Berryhill 1991), although at most locations only two or three are present. These cleavages are interpreted to be shear-related because discrete shear zones with well-defined boundaries contain superposed cleavages that are not present in the adjacent country rock. Superposed cleavages are also observed in larger shear zones where boundaries are not exposed, but the presence of other shear-related kinematic indicators supports a shear-related origin. Hereafter, clockwise younging cleavages found in sinistral zones will be referred to as D_3 crenulations and anti-clockwise younging cleavages found in dextral zones as D_4, following the terminology of Mosher (1983).

154 oriented thin sections have been examined from within and outside the Beaverhead shear zone, of which 70 contain well-developed, superposed crenulation cleavages. The crenulation cleavages are defined by aligned crenulation or microfold limbs (Fig. 2b). For asymmetric crenulations, short limbs define a cleavage domain similar in shape to small-scale kink bands, and the displacement sense across the cleavage domain indicates shortening parallel to the older foliation (Fig. 2c). The cleavages are typically inclined from 42° to 90° to the pre-existing foliation. Those nearly perpendicular to the foliation are generally symmetrical and have rounded hinges, whereas those at angles <80° to the pre-existing foliation are asymmetric and have sharp, kink or chevron shaped hinges. Long limb/short limb ratios generally range from 2 to 10. Angles between microfold limbs, which is a measure of fold tightness, generally range from about 120° to 90° in D_3 crenulations to about 100–75° in D_4 crenulations. Most of the crenulations have micas bent continuously around slightly angular to rounded hinges, although some mica grains exhibit slight microfracturing across hinge regions. Quartz, which generally forms elongate grains parallel with S_1, is smoothly bent around hinges and exhibits wavy to discontinuous undulatory extinction. Both limbs of the crenulations show the same intensity of deformation. All generations of microfolds are generally low to moderate in amplitude and sinusoidal to chevron in shape (amplitude 1–3, fold shape C–E; Hudleston 1973). D_4 crenulations tend to be slightly higher in amplitude and more chevron in shape. Crenulation cleavage spacing, measured perpendicular to the axial planes of adjacent crenulation cleavages in thin section, varies with lithology and crenulation generation. Spacings in the fine-grained graphite schists are about 2 mm and those in the relatively coarse-grained quartz–mica schists are approximately 3–5 mm. Spacings of D_3 crenulations are generally smaller than those of D_4 crenulations, being approximately 1–3 mm rather than 2–4 mm. These cleavages meet none of the criteria used by Platt (1979) to identify extensional crenulations, but instead result from contraction of the foliation.

Overprinting relationships for some cleavages can be determined in the field, particularly if the youngest cleavages are larger or more penetrative, but many are only observable in thin section (Fig. 2). Two main types of relationship are observed: (1) young crenulations fold older cleavages—such folding is easiest to see when cleavages intersect at a moderate to high angle or when young ones are larger; and (2) young crenulations form on only one limb of the older crenulation because the other limb is in an orientation inappropriate for microfolding. This case is most common when the older crenulation is chevron in style and the younger crenulation is at a high angle to one limb of the older crenulation and nearly parallel to the other limb.

Diffusive mass transfer

Gray (1977) proposed that metamorphic differentiation plays a significant role in the formation of crenulation cleavages. For crenulation cleavages (as defined

by Borradaile *et al.*, 1982, p. 5, Ramsay & Huber 1986, p. 436) used in this study to measure shear strains, no change in abundance of any mineral is observed in the hinge or on either limb. Only eight out of the 70 thin sections of superposed crenulations contain thin concentrations of dark material parallel to the crenulation cleavages. Some of these concentrations are accumulations of oxidized biotite, but many are seams of fine-grained opaque material. The seams are discontinuous, generally less than a few mm in length, and increase in number and become closer-spaced in tightened asymmetric folds and near quartz pods. These samples were not used for shear strain measurement. To test for the effects of minor pressure solution that might not be detectable on a microscopic scale, four oriented chips from a sample containing three sets of overprinting crenulation cleavages that did not show seams were examined under the scanning electron microscope (SEM). The cleavages show no truncation of mica grains. Additionally, no quartz accumulations in crenulation hinges nor seams of insoluble material, such as TiO_2, are present. To test for the presence of compositional variations across crenulations that would reflect other diffusive mass transfer processes during microfolding, energy dispersive electron microprobe analyses of micas along the S_1 foliation were undertaken. Deformed white mica in inhomogeneously strained rocks can be systematically enriched in Si^{4+} and depleted in Al^{3+} in the more strained regions (Boulter & Raheim 1974). Probe sections were cut perpendicular to D_3 crenulations because these had the greater probability of involving diffusion than did D_4, being at slightly higher metamorphic conditions (i.e. closer in time to metamorphism). No statistically significant Si^{4+} and Al^{3+} variations are observed in phengites from crenulation limbs and hinges. Thus, neither pressure solution nor diffusive mass transfer was active during formation of the cleavages used for strain measurement, or for most of the crenulation cleavages in the area.

Microfolding strain

Crenulation shapes reflect the amount of shortening by internal buckling of the foliation and bulk flattening of the rocks. The amount of layer-parallel shortening strain that accumulates within the foliation prior to crenulation formation is unknown, although it is assumed to be small because the well-foliated phyllites and graphite schists have ready slip surfaces for microfolding. Determination of buckling accomplished by crenulation involves measurement of crenulation half-wavelengths, where the length measured along the foliation is the undeformed length (l_0) and the length measured along the enveloping surface of the crenulation is the deformed length (l_f) (Mukhopadhyay *et al.* 1969). Shortening measurements were made on 38 oriented thin sections from various locations along and across the Beaverhead shear zone. Measurements were made on photographs, projected thin sections or directly on the microscope stage using an ocular-mounted micrometer. Each thin section was cut exactly perpendicular to a specific crenulation generation and perpendicular to the S_1 foliation. A range in values is observed in a single thin section because crenulation cleavage development is relatively inhomogeneous on the microscopic scale. The values for both D_3 and D_4 buckling strains generally range from 4 to 30%, with most in the 7–15% range (Table 1). Shortening measurements were also made across the few crenulation hinges that showed pressure solution seams. The amount of shortening relative to the adjacent, non-pressure-solved, crenulations varies by no more than 5%.

Flattening across crenulation axial planes can occur during or after buckling and reflects local shape change associated with crenulation as well as any bulk deformation at a scale larger than the crenulations (Gray & Durney 1979). The microstructural, SEM and microprobe observations discussed above indicate that redistribution of material by solid-state diffusion did not occur and that pressure solution occurred only locally and, where present, could be detected in thin section. Thus in most cases, flattening would have to be accommodated by internal distortion of the minerals, most likely quartz, as observed, or slip between micas causing thinning on the limbs. The technique used to determine minimum flattening strains across fold limbs is the t_0/α method of Gray & Durney (1979). This method uses the changes in layer thickness parallel to the axial plane for different limb dips to calculate minimum flattening strains. Fold flattening analyses were conducted on crenulations for 14 samples with approximately 30% quartz and 70% mica using projected thin sections. Minimum flattening strains [$R_{flat} = (\lambda_1/\lambda_2)^{1/2}$] range from 1.1 to 1.5 (5–18%) (Tables 1 and 2). Of those measured, 10 yield flattening strains under 9% and only one was over 12%. Generally, the amount of flattening was asymmetric to the crenulation axial planes, suggesting that the flattening was superimposed during subsequent progressive deformation.

Use as a kinematic indicator

Much recent work has explored the use of planar fabrics as kinematic indicators in ductile shear zones, particularly *S–C* structures in mylonites and, to a lesser extent, extensional crenulation cleavages (Berthé *et al.* 1979, Platt & Vissers 1980, Lister & Snoke 1984, Dennis & Secor 1987). The superposed, non-coaxial contractional crenulation cleavages described above are only found within shear zones and show a consistent clockwise younging in sinistral zones and anti-clockwise younging in dextral zones. Within a single rock, individual cleavage generations with the same overprinting relationships (e.g. clockwise) are similar in morphology, scale, spacing, geometry, definition, etc. These similarities and their presence in shear zones suggest that they formed sequentially during progressive non-coaxial deformation within shear zones. (See a similar argument for multiple extensional crenulation cleavages: Platt & Vissers 1980.) Thus, these cleavages can also be used as

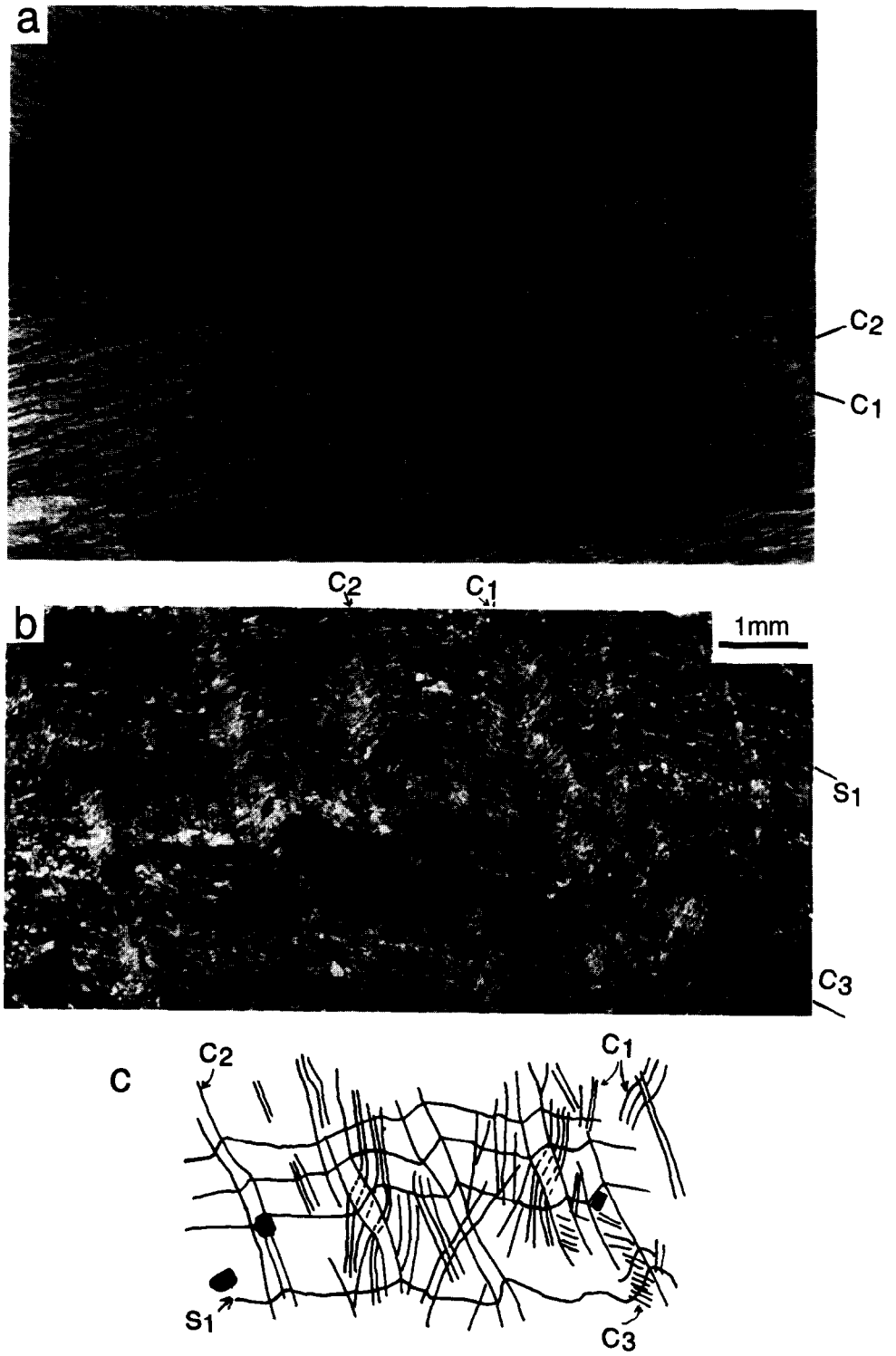

Fig. 2. (a) Superposed crenulation cleavages on the pre-existing foliation (S_1) surface. C_1—First-formed cleavage, C_2—second-formed cleavage at a slight angle; anti-clockwise younging indicated. Photograph width is 20 cm; outcrop view perpendicular to S_1. S_1 changes orientation slightly in upper right and upper left. (b) Superposed crenulations in thin section. C_1—First-formed crenulation cleavage; C_2—second-formed; C_3—third-formed. Note spacing between cleavages and the consistency in orientation of C_1 and C_2 cleavages despite the interference. C_1 has generally rounded hinges and is nearly perpendicular to S_1; C_2 has kink-like hinges and is oblique to S_1. Photograph taken in cross polars; thin section is perpendicular to S_1 and C_2. (c) Sketch of (b) showing interference of C_1 and C_2; C_3 only shows up on one limb of C_2. C_1 cleavages can be traced through C_2 cleavages as the stage is rotated.

Table 1. Shear and buckling strains, orientations of pre-existing foliation, superposed crenulation cleavages and calculated shear strains and angular relationships

Sample	Strike and dip of S_1	Strike and dip of C_1	Strike and dip of C_2	ϕ	α	v	p	p'	γ	Shear sense	Strike and dip shear plane	Buckling strain
Beaverhead												(flattening*)
B 13	161 30E	358 60E	33 55E	66	10.5	0	84	9	6.2	s	352 51E	(R_s = 1.5)
BB 11	1 8E	298 65W	336 71W	80		0	43	7	7	s	290 65W	
BB 1	5 30E	315 62W	357 54W	83		0	44	7	7.1	s	306 65W	
BB 15	15 52E	171 32W	303 53W	81		2	43	5	10.3	d	2 31W	8–11
BB 2	41 26E	324 68W	321 66W	72	21	35	64	60	0.11	d	12 78E	9–15
12.2	8 29E	334 64W	14 63W	88		0	45	9	5.3	s	323 65W	10–12
B 63	21 20E	28 75W	65 80W	88		0	45	8	6.1	s	19 76W	15–17
BB11a	19 3E	307 70W	328 46W	48	0	48	63	33	1.5	s	290 81E	13–22
7.1	323 23E	359 90	35 88W	85		6	47	10	4.8	s	349 90	
8.1	359 12E	17 90	45 89W	80		2	45	17	2.3	s	0 89E	12–17
BB 19	77 88E	77 35E	23 12E	82		3	40	10	4.5	d	83 46N	15–19
Dutch Island												
DI 1a	33 26E	2 78W	11 38W	42	0	27	88	64	0.5	s	0 79E	10–12
DI 1a	33 26E	11 38W	21 16W	42	0	27	64	24	2	s	0 79E	10–14
27–1	36 41E	8 75W	20 71W	69	16	54	26	14	3.3	s	5 80W	10–15
R7	23 35E	9 64W	28 62W	83		0	45	27	1	s	340 72W	10–12
Du 9	37 16E	312 75W	295 82W	79	0	48	40	22	1.9	d	335 68W	7–9
Du 30	339 22E	7 82W	17 66W	84		0	50	30	0.9	s	352 72E	5–8
R4	40 56E	28 62W	9 64W	67	12	49	22	4	18	d	33 62W	21–30
R2	43 45E	35 65W	5 60W	83		0	41	13	3.2	d	49 70W	17–19
Gould Island												
G5	350 48E	130 60W	98 45W	72	21	20	80	50	0.7	d	346 84E	5–7
GB 5	13 30E	15 58W	339 67W	88		1	46	14	3	d	32 57W	
GID	344 36E	0 59W	388 58W	86		2	46	20	1.8	d	31 65W	
GA 4	357 46E	348 41W	26 35W	78	30	60	46	22	3	s	326 56W	(R_s = 1.1)
SK 2	27 23E	349 73W	16 68W	90		1	45	20	1.7	s	331 80W	5–9
GI7-1	62 46E	33 57W	45 46W	90		0	45	30	0.7	s	15 83W	
GI 5–13	306 36W	18 71E	336 59E	88		0	46	7	7.2	d	24 74E	8–10
SK 3	11 12E	336 60W	4 87E	76	27	34	80	32	1.7	s	301 40WS	8–11
G11-3	37 52E	347 46W	329 76W	82		1	46	12	3.7	d	358 37W	5–10
GB5-2	13 24E	326 52W	1 42W	66	10.5	51	36	9	7.8	s	317 58W	
G-4	338 52E	287 71W	278 45W	80		0	53	25	1.4	d	293 84E	6–10
GI 5–9	9 30E	359 42W	36 42W	70	17.5	59	26	2	51.6	s	358 42W	(R_s = 1.3)
GI 5-14	35 34E	331 76W	325 44W	63	5	18	74	42	0.9	d	338 61E	
Eastern, central, western Rhode Island												
BG 1b	355 50E	343 45W	358 39W	90		0	44	32	0.6	s	313 70W	
CD 2	337 30W	23 80W	38 70W	59	0	48	34	16	3	s	10 90	
CD 3	278 18W	47 64W	53 54W	65	26	46	79	68	0.3	s	20 53E	4–7
PA 10	61 17E	100 90W	308 86W	80		12	43	16	2.5	s	85 88N	
PA 16	59 15E	73 58W	80 48W	62	3.5	15	75	64	0.2	s	50 62E	
FR-1	355 29E	333 73W	341 63W	89		0	45	33	0.5	s	314 80E	
FR	357 28E	357 65W	341 63W	90		1	44	30	0.7	d	27 73W	
SF 3	21 26E	5 89W	340 70W	90		2	45	14	3	d	17 82E	
BS 5.3	7 66E	346 21W	10 18W	83		9	44	36	0.3	s	307 50W	7–10
204-5	12 50E	358 32W	15 34W	85		1	42	33	0.4	s	305 43W	8–12
207 B-1	350 49E	287 30W	333 33W	81		1	40	17	2	s	80 36S	6–9

*Where not given in Table 2.

Table 2. Shear, flattening, buckling and total strains for representative samples

Sample No.	γ	Flattening strain (R_s)	Buckling strain (%)	Total strain (%)
BB2	0.11	1.3	10–12	30.6–32.5
B63	6.00	1.2	13–22	27.5–35
BI1a	3.25	1.2	10–12	24.9–26.9
Du9	1.30	1.2	7–9	22.5–24.2
R4	12.00	1.3	21–24	37.5–41.7
R2	3.50	1.1	17–19	24.2–26.4
Sk 2	1.90	1.2	5–9	20.8–24.2
Sk 3	1.60	1.2	8–11	23.3–25.8

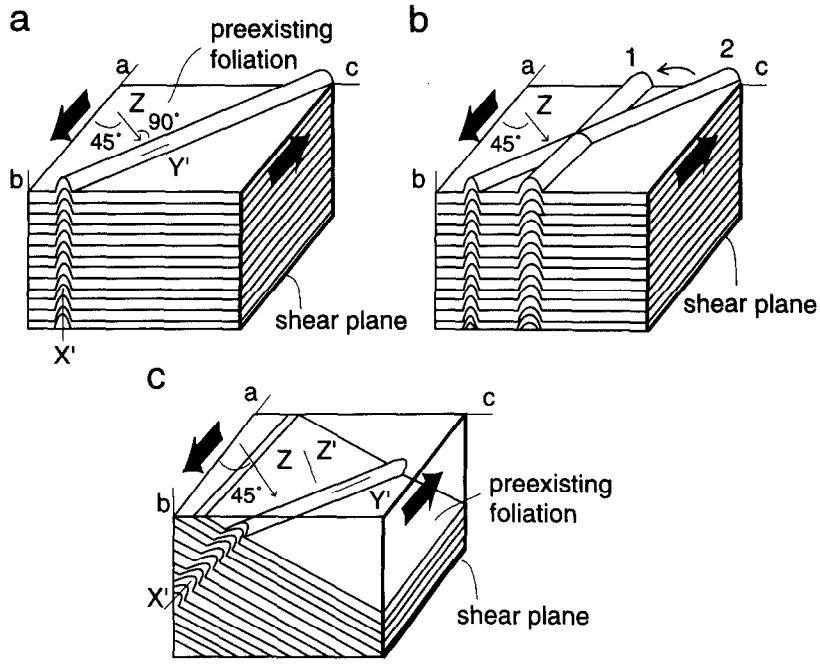

Fig. 3. (a) Horizontal pre-existing foliation in a vertical sinistral shear zone. Foliation lies within the *ac* plane which contains the *XZ* plane strain ellipse for simple shear; *Z* shown at 45° to shear zone. A vertical crenulation cleavage forms perpendicular to the shortening direction (*Z*). The maximum extension direction for crenulation cleavage (*X'*) is parallel to *b* and not to the *X* direction of the simple shear plane strain ellipse. (*X'*, *Y'* denote the axes of the incremental strain ellipsoid recorded by the crenulation cleavage.) (b) Same shear zone as in (a) but after rotation of the first cleavage and formation of the second. The direction of rotation and relative age are indicated. Note that clockwise younging results from sinistral shear. The crenulation appears narrower before rotation because the view is oblique. (c) Pre-existing foliation inclined to the *ac* plane in a vertical sinistral shear zone. The crenulation cleavage forms at a high angle to the foliation and not parallel to the *b* direction. No incremental strain axes coincide with those of the simple shear system. (*Z*—incremental shortening direction for the shear zone; *X'*, *Y'*, *Z'*—incremental strain ellipsoid axes recorded by the crenulation cleavage.)

a kinematic indicator (Berryhill 1984, Burks 1984, 1985, Mosher & Berryhill 1991).

FORMATION OF SUPERPOSED CRENULATIONS

The superposed contractional crenulation cleavages described above form in nearly vertical shear zones on a nearly flat-lying metamorphic foliation. Thus, the pre-existing anisotropy is essentially parallel to the *ac* plane (i.e. perpendicular to the *b* kinematic direction and to the shear (*ab*) plane) (Fig. 3a). Under conditions favorable for folding rather than fracturing, buckling of the foliation forms folds perpendicular to the shortening (*Z*) direction of the incremental strain ellipsoid. Ideally the crenulation cleavages should form at 45° to the shear plane (perpendicular to the shortening direction), and cleavage should be perpendicular to the pre-existing foliation.

After formation, the crenulation cleavages rotate towards the shear plane as semi-passive markers; that is they may continue to amplify during deformation but the fold hinge lines themselves rotate as essentially passive linear markers (Flinn 1962). This assumption of passive rotation rather than active hinge migration (Treagus & Treagus 1981) is justified for the kink-like crenulations because the sharp hinges would inhibit hinge migration. For the round-hinged crenulations, the presence of superposed sets of crenulations indicates that active hinge migration, if present, was insufficient to accommodate the progressive strain. Thus, the effects of active hinge migration should be negligible in comparison to that of passive rotation. The alignment of hinge lines and adjacent microfold limbs across adjacent layers defines the crenulation cleavage. Consequently, the cleavages should also rotate as essentially passive planar markers. Such structures that remain strain-sensitive for only a portion of their history can be treated the same as the 'so-called passive markers' of Ingles (1985) that deform during deflection (e.g. pre-existing dikes).

At some point in the rotation of these crenulation cleavages, they will no longer be suitably oriented with respect to the incremental shortening direction to accommodate the strain by buckling. Once buckling stops, these crenulations become 'locked' and may rotate as completely passive markers or may undergo extension parallel to microfold axes. For the crenulations measured in this study, no microstructural evidence of extension parallel to the crenulation axes was observed. Bulk extension in this direction is recorded locally by boudinage and multiple sets of cross-cutting veins, but no extension on the scale of the crenulations or in the outcrops sampled is observed. Instead, one or more additional crenulation cleavages were superposed on the first cleavage at a small angle (Fig. 3b). This superposition suggests that if deformation continues

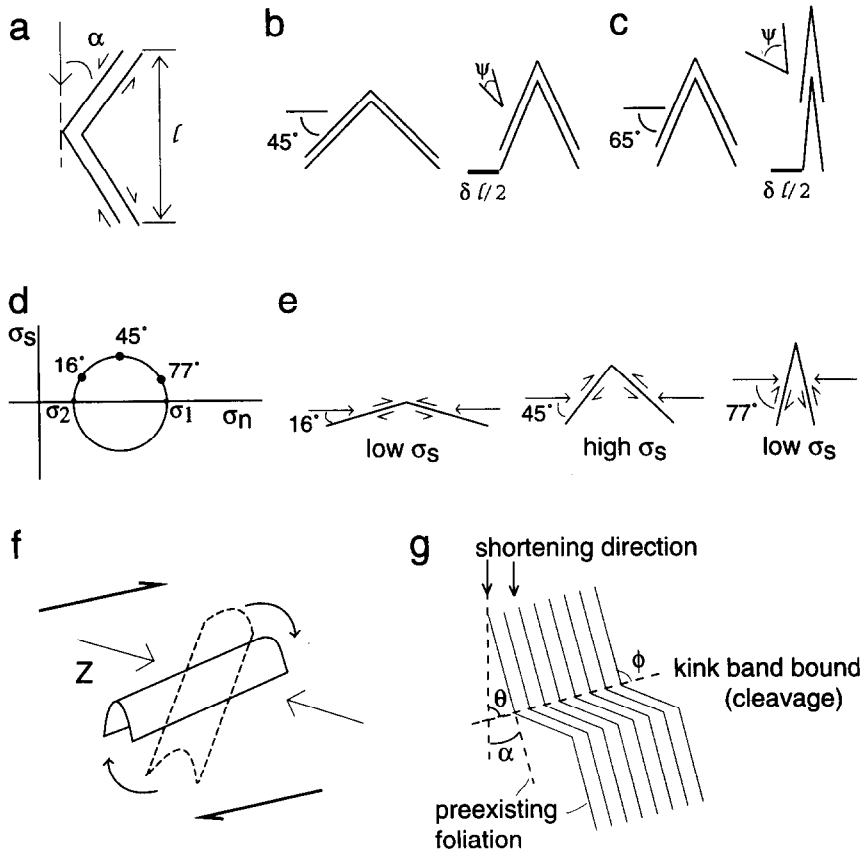

Fig. 4. (a) Chevron fold with shear sense on limbs as shown. α—Angle between the shortening direction and the pre-existing foliation; l—original wavelength. (b) & (c) Two chevron folds before and after equivalent shortening of δl. Initial angles of (b) $\alpha = 45°$, (c) $\alpha = 65°$. The thick horizontal line represents $\delta l/2$. Layer thickness on limbs and line lengths are maintained; amount of layer offset after shortening represents shear strain between layers on the limbs. The magnitude of angular shear strain (ψ) between limbs during folding is indicated. Note that for equivalent shortening, chevron folds with larger α values undergo more angular shear strain. (d) Mohr circle for stresses with relative stresses for planes at 16°, 45° and 77° from σ_1 indicated. (e) Three chevron folds with angular relationships between σ_1 and limbs corresponding to those indicated on the Mohr circle in (d). Note that the highest shear stress occurs on limbs at 45° to σ_1. (f) Rotation of a fold in a dextral shear zone causing a decrease in angle between the shortening direction and the fold limbs. Dashed line—initial fold position; solid line—position after rotation. (g) Angular relationships between pre-existing foliation, shortening direction and kink band boundary (after Gay & Weiss 1974). Note that the shortening direction and poles to the pre-existing foliation and the kink band boundary lie in the same plane.

after the crenulations lock, a second generation of cleavages may form to accommodate the continued shortening. This generation will have the same initial geometry relative to the shear zone boundary as the first, assuming the first cleavage does not have any mechanical effect (see below). With continued deformation, the second cleavage may also rotate until it cannot accommodate further strain by buckling, and a third cleavage may initiate, and so on. Each sequential cleavage generation should rotate in a similar manner to the first-formed shear-related cleavages because they are all mechanically-identical fabric elements. The number and three-dimensional geometries of superposed crenulation cleavages should be a function of the amount of shear strain, strain rate, lithology and precise orientation of the pre-existing foliation relative to the shear plane. The observed superposed cleavages show consistent overprinting relationships that indicate younging in a clockwise direction in sinistral zones or an anti-clockwise direction in dextral zones. This sense of younging is consistent with formation in a shear zone as described above. Thus, younging sense can be used to determine the relative movement directions across individual ductile shear zones.

The model given above requires that the microfolds become 'locked' and cease to accommodate the strain with rotation. The most likely explanation for the 'locking' is that crenulation of the thin mica folia is analogous to chevron or kink folding (see Ramsay 1967, pp. 436–456). As a chevron fold amplifies, the amount of shear strain between layers per increment of shortening strain across the fold is at a minimum at angles of $\alpha = 30$–$40°$ (angle between shortening direction and layer) and increases nearly exponentially with increasing angles of α (Figs. 4a–c) (Ramsay 1967, p. 442, fig. 7–113). Thus, chevron folds tend to lock (or the rate of shortening decreases) with increasing amplitude because more slip must occur between layers for each increment of shortening across the fold. Another contributing factor to locking of chevron folds is the change in shear stress across the layers during amplification. If the maximum compressive stress is parallel to the shortening direction, the shear stress across the layers is a maximum at $\alpha = 45°$ and decreases with increasing or decreasing α (Figs. 4d

& e). Thus, chevron folds tend to lock as they amplify past $\alpha = 45°$, because the shear stress becomes too small to cause slip. These two factors combine to cause chevron folds to lock with increasing α (and decreasing interlimb angles). Less shear stress is available to cause slip between layers, and the amount of shortening that results from slip between layers is significantly less.

In the case of shear zones, an additional factor is involved. The normal to fold axial plane rotates progressively away from the shortening direction, and the angle between the fold limbs and the shortening direction decreases (Figs. 3b and 4f). Thus, the amount of shear stress across the layers decreases. (Note that this effect will occur at some point during the rotation even though the maximum compressive stress is at an angle to the maximum shortening direction.) The final interlimb angle of the folds should depend on the rate of rotation relative to the rate of amplification (cf. Ridley 1986). In general, the combination of rotation and amplification should cause such folds to lock with larger interlimb angles (lower α) than those undergoing coaxial strain. This prediction is supported by the field observations. The interlimb angles of the superposed crenulation cleavages are larger than the usual ~60° observed for chevron folds. As the folds amplify during rotation, the amount of shortening that can be accommodated by further amplification also decreases. Thus, not only is the fold no longer favorably oriented relative to the incremental shortening direction, but it is also starting to lock and ceasing to have the mechanical ability to accommodate the strain. It is easier to form a new crenulation cleavage that is ideally oriented than to accommodate the incremental strains.

Mechanical effect of early crenulation cleavage

Before the angular relationships between superposed crenulation cleavages can be used to quantify the amount of incremental rotation, the mechanical effect of the first-formed crenulation cleavage on the formation of a second must be explored. Several observations indicate that the crenulation cleavages do not act mechanically as planar anisotropies. In the Narragansett Basin metasedimentary rocks, the pre-existing metamorphic foliation is a very strong mechanical anisotropy that is never destroyed or obscured regardless of the amount of deformation. The crenulations are defined by a reorientation of this anisotropy and are not associated with solution seams, mica-rich bands, or other new features that would cause a new mechanical anisotropy. The crenulations are not as penetrative as the pre-existing foliation. In most rocks the microfolds occur in thin, discrete domains (e.g. 0.5 mm) separated by much wider domains (e.g. 2.5 mm) of unaffected planar foliation (Figs. 2b & c). Young ones crenulate the foliation and cut across the older ones with little to no change in orientation within the thin microfold domain. Cleavage measurements are taken from the wide domains where the foliation is planar; thus even a minor effect is avoided. In cases where the orientation of one limb of chevron-shaped crenulations is inappropriate for microfolding, younger crenulations form only on the other limb and die at the hinges. Only the continuity, not orientation, of younger crenulations is affected. Crenulations of the same set (i.e. D_3 or D_4) do not occur at a high angle to one another; therefore, the few closely-spaced chevron microfolds do not show different orientations of younger crenulations on opposite limbs. If this did occur, the cleavage would be unusable.

Another factor to consider is whether pre-existing crenulation lineations form a pre-existing linear anisotropy that controls the orientation of new lineations. A few physical models in the literature indicate that pre-existing folds will inhibit the formation of new folds at a small angle to the pre-existing ones. For example, Ghosh & Ramberg (1968) modeled superposed folds in compression using a single layer of modeling clay. When the compression axis was at 30° to the first set of folds, no new folds formed. Instead the old folds increased in amplitude and rotated. In the experiment, the strain could be accommodated by the rotation and growth of the folds, thus a new set was not needed. Nonetheless, careful examination of the experimental results (Ghosh & Ramberg 1968, plate IV) shows a possible faint new set of fold axes perpendicular to the shortening direction that in a few places distorts the pre-existing folds. Their experiment is not analogous to the present situation, however, because during non-coaxial deformation, the normal to fold axial planes rotates away from the incremental shortening direction. Thus, the folds may rotate into a position where they can no longer accommodate the strain. A more analogous model is that of Odonne & Vialon (1983) who modeled folding over a basement wrench fault using paraffin wax. With small displacements, folds formed at about 45° to the shear plane. With large displacements, new folds formed parallel to the old rotated ones, indicating that the old ones created a controlling linear anisotropy. This model was not scaled for microfolding and the scale dependence of the results is not known. Perhaps more importantly, the model was not set up to simulate chevron/kink folding. Thus, the model results may not be applicable to the present study. Other unscaled experimental models and field observations (Cobbold & Watkinson 1981, Watkinson & Cobbold 1981, Watkinson 1983) have shown that rigid linear markers imbedded in a more ductile layer, such as quartz fibers in nature, will affect the orientation of crenulations in the overlying foliation. The earlier crenulations are not rheologically different than the rest of the rock, thus such a pronounced effect should not occur. Also thin sections of crenulations clearly demonstrate that they are crenulations and not ripples over quartz fibers.

The presence of superposed crenulation lineations and cleavages proves that older ones did not inhibit the formation of younger ones at a small angle (<30°). Field observations also argue against the lineations and cleavages controlling the orientation of younger ones. Each generation is not pervasive across an entire area. In many locations, one crenulation can be tracked across a

large area with a homogeneously dipping pre-existing foliation where the number of earlier crenulation generations varies. The lineation and cleavage orientation is consistent regardless of the presence or absence of older crenulations (see Mosher & Berryhill 1991, fig. 10). This observation strongly supports the contention that the crenulation lineations and cleavages do not impart any linear or planar mechanical anisotropy to the rock which might affect the angle of formation of the subsequent cleavages.

Effect of pre-existing foliation

Formation of a cleavage by crenulation of a pre-existing foliation (anisotropy) results in a special situation where the orientation of the anisotropy relative to the shortening direction controls the incremental strain ellipsoid recorded by the crenulation cleavages, and thus the resultant finite strain ellipsoid (Flinn 1962). If the pre-existing foliation in a shear zone is parallel to the *ac* plane, it will contain the shortening (Z) direction of the incremental strain ellipsoid (Fig. 3a). In this case, the crenulation cleavages should form at 45° to the shear plane (perpendicular to the shortening direction) and perpendicular to the pre-existing foliation. The buckling will cause elongation parallel to the *b* kinematic direction. Extension along the fold axes will generally be much less. Therefore, the maximum elongation (X') direction for the incremental strain recorded by the crenulation cleavage will be parallel to the *b* direction. Thus, the effect of the pre-existing anisotropy will be to change the simple-shear-induced plane strain, where the X direction lies in the *ac* plane, to one of triaxial strain, where X is perpendicular to the *ac* plane.

If the pre-existing anisotropy in a shear zone is inclined relative to the *ac* plane, but still at a high angle to the *b* kinematic direction (Fig. 3c), none of the axes of the incremental strain ellipsoid recorded by the crenulation cleavage will coincide with those for the shear zone. For the incremental strain recorded by the crenulation cleavage, the elongation direction (X') will be at a high angle to the foliation (not parallel to *b*), and Y' will be within the foliation parallel to the crenulation axes. The maximum shortening (Z') direction recorded by the crenulation cleavage will be perpendicular to the crenulation cleavage, not parallel to the shortening direction (Z) for the shear zone. The orientation of the crenulation cleavage, and thus the recorded incremental strain, will be controlled by the inclination of the pre-existing foliation relative to the shortening axis.

Although the pre-existing foliation in the study area was generally parallel to the *ac* plane, the effect of slight to moderate inclinations must be considered when evaluating the orientation in which crenulations form as well as any subsequent rotation of the pre-existing foliation during progressive simple shear. The relationship between the orientation of kink bands and the inclination of the preexisting foliation relative to the shortening direction has been well documented by experimental studies. This relationship can be used in this study for the cases in which the pre-existing foliation is inclined to the *ac* plane and resultant crenulations have a kink-like geometry. The most extensive study was that of Gay & Weiss (1974) who tested 123 slates at initial angles between 0° and 30° to the shortening direction. They found a linear relationship between initial inclination of the foliation to the shortening direction (α) and the angle between the external foliation and the kink bands (ϕ) (see Fig. 4g). The equation for the best-fit line of their data is $\phi = 60 + 0.57\alpha$. Tests of card decks (Gay & Weiss 1974) showed that at inclinations greater than 15°, sliding along the foliation occurred. At angles greater than 30°, sliding should dominate and kinks should not form. The results of Gay & Weiss (1974) are compatible with previous experimental data (e.g. Donath 1968), and these authors proposed that the linear relationship between foliation inclination and kink band orientation can be used in natural samples to find the shortening direction. The linear relationship between α and ϕ is only valid within the range of values tested. More recent experiments by Williams & Price (1990), done in simple shear, are not applicable to the present situation. In those experiments, as in the modeling of Dennis & Secor (1987), the pre-existing foliation was parallel to the *b* direction whereas in the present case the pre-existing foliation is nearly perpendicular to the *b* direction.

SHEAR STRAIN MEASUREMENT

Methods

The model discussed in the previous section for formation and rotation of superposed crenulation cleavages in shear zones (Figs. 3a & b) allows the angular relationship between superposed crenulation cleavages and between the last-formed crenulation cleavage and the shear zone to be used to quantify the amount of incremental rotation, and therefore, incremental shear strains, recorded by the crenulation cleavages. If the pre-existing foliation lies within the *ac* plane, a two-dimensional approach can be taken (Fig. 5). To treat the more generalized geometric case where the pre-existing foliation is inclined to the *ac* plane of the shear zone (Fig. 3c), a three-dimensional geometric approach is needed. In this more general case, the mechanical effect of the pre-existing foliation must be considered.

In two dimensions, crenulation lineations can be treated as passive material lines which will rotate toward the shear plane as a function of increasing shear strain. After the crenulations rotate into an orientation where they can no longer accommodate the incremental strains, a new generation will form at some angle to the previous generation. For each increment of strain, the amount of rotation of each lineation will vary with orientation relative to the shear plane, and the dihedral angle between two lineations will decrease with increasing shear strain. If the pre-existing foliation within a vertical, strike-slip shear zone is horizontal (i.e. parallel

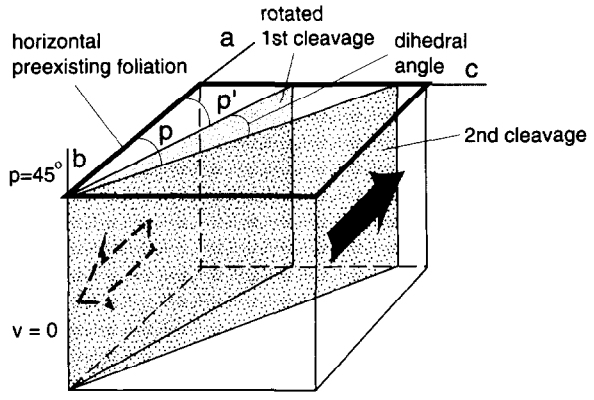

Fig. 5. Horizontal pre-existing foliation in a vertical sinistral shear zone showing rotated position of first-formed and initial orientation of second-formed crenulation cleavages. The intersection of two cleavages parallels the b direction ($v = 0$), p is the angle between the second cleavage and the shear zone, and p' that between the rotated first cleavage and the shear zone. In two dimensions, the dihedral angle on the pre-existing foliation reflects the amount of shear strain that occurred between formation of the two cleavages.

to the ac plane), the angle between two superposed crenulation lineations should be a measure of the incremental shear strain. The crenulation cleavage, itself, is perpendicular to the pre-existing foliation and contains the b direction (Figs. 3a and 5). Using equations describing homogeneous progressive simple shear, the rotation of lineations from the initial (α) to the deformed angles (α') as a function of shear strain (γ) is: $\cot \alpha' = \cot \alpha + \gamma$ (Ramsay 1967, p. 88). The difference between the shear strains calculated for two successive crenulation lineations, assuming some initial angle to the shear plane, gives the incremental shear strain that occurred prior to the formation of the younger crenulation lineation. The error introduced by assuming an incorrect initial angle (i.e. 45° rather than 41°) is small. For example, a dihedral angle of 25° yields a shear strain of 2 ± 0.3. The amount of shortening (expressed as $1 + e_3$) along the foliation that should accompany a given amount of simple shear is given by: $\lambda_3 = 1/2\,[\gamma^2 + 2 - \gamma(\gamma^2 + 4)^{1/2}]$ (Ramsay 1967, p. 85) where $(1 + e_3) = \lambda_3^{1/2}$. If crenulations record more strain than could result from simple shear, then pure shear or volume change must have acted in addition. If less strain is recorded, then the strain must have been accommodated by additional processes such as mesoscopic folding or active hinge migration.

In three dimensions, the rotation of planar structures as a function of shear strain in progressive simple shear can be described using geometric models and equations for homogeneous deformation given by Skjernaa (1980). These equations can be extended and modified to calculate the incremental shear strains recorded by each sequentially formed crenulation cleavage if the orientations of the shear zone boundary and cleavages are known. The three-dimensional rotation of a plane within a vertical, sinistral ductile shear zone is illustrated in Fig. 6. The orientations of the deformed and undeformed planes relative to the kinematic axes (a, b, c) are described using two parameters, v and p, where v is the angle between the b direction and the trace of the plane on the shear plane and p is the angle between the plane and the shear plane. As the plane rotates, the trace of the plane on the shear plane acts as an imaginary hinge, thus v remains constant during deformation. The angle between the plane and shear plane changes from p in the undeformed state to p' in the deformed state. From these parameters, the shear strain can be calculated using the equation: $\gamma = [|\tan(p' - 90) - \tan(p - 90)|]/|\cos v|$, (Skjernaa 1980). Figure 7 shows a theoretical plot of $p - p'$ vs γ for various initial v and p values. Note that γ is relatively insensitive to changes in v for a given p but is sensitive to changes in p for a given v.

In the case of superposed crenulation cleavages, the first-formed cleavage is rotated toward the shear plane until the crenulation 'locks' and a second cleavage forms. The second cleavage should form in the same orientation that the first cleavage had formed, if the pre-existing foliation has not changed orientation. (See later section on effects of pre-existing foliation for justification.) Thus, the second cleavage marks the initial orientation of the older cleavage. The intersection of the two cleavages will lie within the shear plane and have the same angle v. The angle between the shear plane and the first cleavage is p and that between the shear plane and the second cleavage is p' (Fig. 5).

In the Narragansett Basin shear zones, shear zone boundaries, where exposed, are not sharp planar features, and it is not possible to measure their orientation with the accuracy required. Also, many shear zones contain large-scale, shear-related structures that formed after the crenulations (Mosher & Berryhill 1991), which may have reoriented the rock containing them relative to the present shear zone boundary. For these reasons, the orientation of the shear plane must be determined using the available data. The orientation of the shortening direction for each cleavage–foliation pair can be calculated using the angle (ϕ) between the last-formed crenulation cleavage and the pre-existing foliation (Fig. 4g), provided that the angular relationships among the pre-existing foliation, the last-formed crenulation cleavage and the shear plane have not been modified significantly by subsequent shearing. For crenulation cleavages used in the present study, ϕ varies between 42° and 90° with symmetrical, round-hinged buckle folds where $\phi = \sim 90°$ and asymmetrical, kink-like folds where $\phi < 80°$. For both cases, the shortening direction will lie on the plane containing the poles to the pre-existing foliation and the last-formed cleavage plane. For symmetrical, round-hinged buckle folds, where the foliation and last-formed cleavage are nearly perpendicular (80–90°), the shortening direction is 90° from S_1, essentially parallel to the pole to the last-formed cleavage (Fig. 8a). This assumption is appropriate for ϕ as low as 80° because Treagus & Treagus (1981) have shown that a 10° or less inclination of a plane relative to the shortening direction has an insignificant effect on the orientation of a developing fold. For asymmetrical, kink-like folds, where the angle (ϕ) is smaller, the angle between the foliation and the shortening direction is calculated using the equation for the best-fit line of Gay & Weiss (1974).

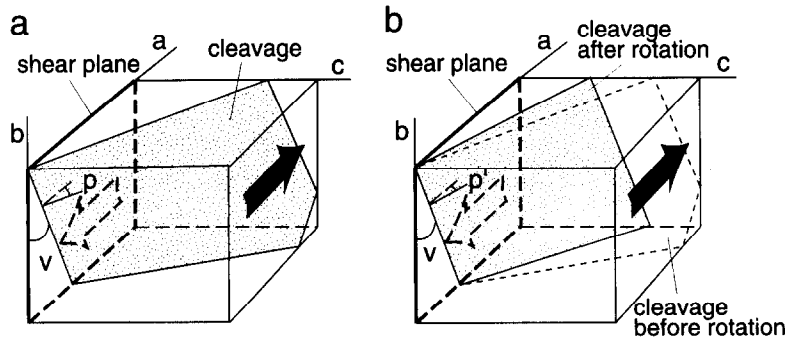

Fig. 6. Generalized rotation of planes in a vertical sinistral shear zone; v, p and p' indicated (modified from Skjerna 1980).

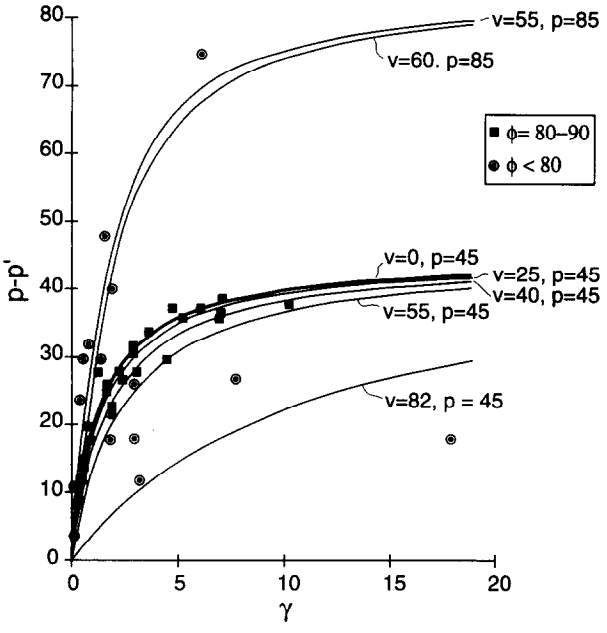

Fig. 7. Plot of theoretical curves for $p - p'$ vs γ for various values of v and p and of data for cleavages used in this study. The theoretical curve for $v = 0°$, $p = 45°$ is thicker. Note that cleavages with $\phi = 80$–$90°$ fall closest to this line whereas those with $\phi < 80°$ fall farther away.

The shortening direction will be at an angle of $(90-\theta)°$ from the pole to the cleavage and $(90 - \alpha)°$ from the S_1 pole, where $\theta = \phi - \alpha$ (Fig. 8b). In both cases the shear plane must be 45° from the shortening direction, contain the intersection of the two crenulation cleavages, and show the correct sense of shear. This shear plane can be found by plotting the cone of shear plane poles at 45° to the shortening direction and then finding which two poles define planes that contain the intersection of the two crenulation cleavages. Only one of the two possible shear planes predicts the correct overprinting relationships (i.e. sense of shear) (Fig. 8). Once that shear plane is known, the values of p, p' and v can be read off the stereonet and the shear strains calculated. (p—angle between shear plane and last-formed crenulation cleavage; p'—angle between shear plane and first-formed crenulation cleavage; v—angle between intersection of two crenulation cleavages (lies on shear plane) and b direction.)

For the calculations, we have assumed the shear zone is pure strike-slip (b direction within shear plane and perpendicular to shear plane strike). Most independent kinematic indicators (e.g. en echelon folds and veins, slickensides on parallel faults, deflection of structures, sheath folds, fibrous veins, superposed large-scale folds, etc.) for the zones used indicate that the component of oblique slip is minor. In the cases where $\phi = \sim 90°$, the intersection of S_1 (nearly parallel to ac plane) and the shear zone (ab plane) give approximate values for a and therefore b. Using these cases as a check, we found that an assumption of pure strike-slip causes b to be mislocated along the shear zone by less than 10° and usually only a couple degrees, affecting the measured v value. Shear strains are insensitive to changes in v if $v < 50°$ because cos v is used to calculate shear strains. The effect of different v is shown in Fig. 7 where $p-p'$ vs γ is plotted for a constant $p = 45°$ and v ranging from 0° to 82°. Values of v from 0° to 40° essentially plot on top of one another. Results for $v = 55°$ plot only slightly lower than the others. By a $v = 82°$, the difference is significant. On Fig. 7, the shear strain error caused by an incorrect v (i.e. $v=0°$ instead of $v = 25°$) is equal to the horizontal separation between curves with the same p (i.e. $v=0°$, $p=45°$ and $v = 25°$, $p=45°$). For $\gamma < 10$, even large errors (<40°) in v result in minor errors in shear strain. Thus any errors in v caused from choosing an incorrect b orientation will be negligible if $v < 50°$. For example, the case shown in Fig. 8(a) has an error in v of 14° if pure strike-slip is assumed, the largest error observed for our data set. The error changes the shear strain from $\gamma = 6.3$ to $\gamma = 6.1$. We have assumed pure strike-slip for all cases because the location of b cannot be determined precisely for $\phi < 80°$.

The angle between superposed crenulation cleavage planes ($p - p'$) reflects the amount of rotation of the first-formed cleavage plane. The amount of rotation varies with the angle (v) between the b direction and the intersection lineation of the cleavage plane and shear plane. This intersection lineation (which parallels the intersection lineation of the two sequential cleavages) will not parallel the kinematic b direction (v not equal to 0) if the pre-existing anisotropy, which controls the orientation in which the cleavage initiates, is inclined relative to the ac plane. For the same dihedral angle ($p - p'$) and initial p, a cleavage plane pair whose rotation axis is parallel to the b-axis ($v = 0°$) involves significantly less shear strain than does a cleavage pair whose rotation axis is at a high angle to the b-axis (Fig. 7). Thus, unlike the restricted two-dimensional model of crenulation

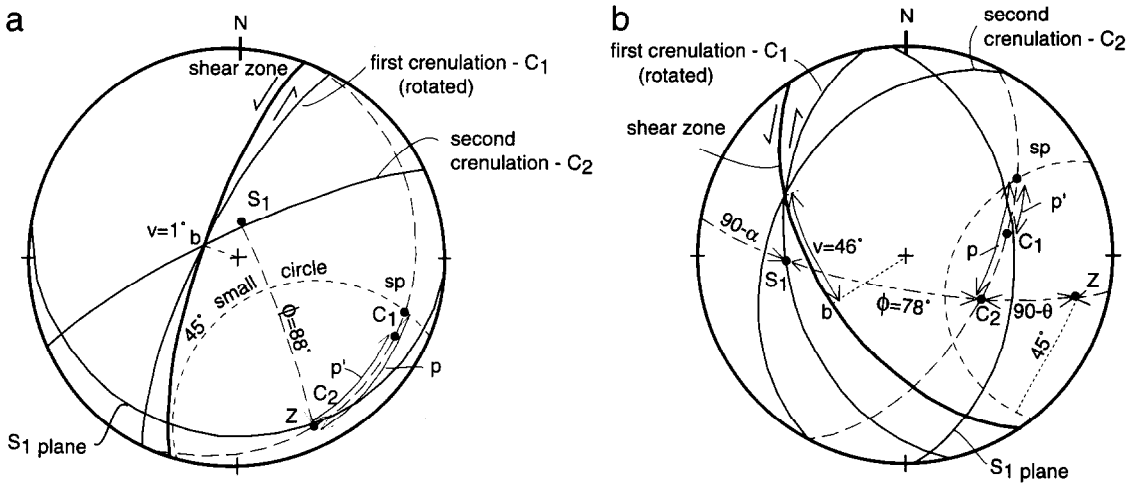

Fig. 8. Equal-angle, lower-hemisphere stereographic projections showing relationships used to calculate shear strains. Z lies on the great circle containing the poles to S_1 and C_2, 90° from the pole to S_1 for ϕ = 80–90°, and 90° − θ from C_2 and 90° − α from S_1 for ϕ < 80°. The 45° small circle contains all possible poles to shear zones for shortening direction (Z). The intersection of two cleavages lies within the shear plane and is 90° from the plane containing the cleavage poles (long dashed line). The intersections of this great circle and the 45° small circle mark the only two possible shear plane poles that contain the cleavage intersection line. Only one (sp) gives the correct sense of shear for cleavage superposition. Angle v equals the angular distance measured along the shear plane from the cleavage intersection to the b direction (within the shear plane perpendicular to the strike of the shear zone); p equals the angle between C_2 and sp; p' equals the angle between C_1 and sp. (a) Case where ϕ = 88°. Z is 2° from C_2; v = 1°, p = 45°, p' = 8°; γ = 6.1. Sample B63. (b) Case where ϕ < 80°. ϕ = 78°, α = 30°. Z is 90° − θ from C_2 (48°) and C_2 is ϕ (78°) from S_1; v = 46°, p = 46°, p' = 22°; γ = 2.2. Sample GA4.

axes, the great-circle angular distances between successive cleavages ($p - p'$) are not direct measurements of incremental shear strain. In this paper we have used the three-dimensional geometric approach for all shear strain calculations.

Effect of pre-existing foliation

If the pre-existing foliation is oblique to the *ac* plane, it will also rotate during deformation, changing position between the formation of the two crenulation cleavages (Figs. 9 and 10). In this case, the second-formed crenulation cleavage will not mark the initial position of the first-formed cleavage, and the intersection of the two crenulation cleavages need not lie in the shear plane. Because this intersection is used to find the shear plane, any calculated shear strains are in error. The strike and dip of the pre-existing foliation relative to the *ac* plane (or v and p relative to the shear plane) determine how much it rotates for a given shear strain. It is the angle (α) between the pre-existing foliation (S_1) and the shortening direction, however, that determines the orientation at which the crenulation cleavages form. Thus the amount of rotation of S_1 does not directly correspond to a change in α. For example, a large rotation of S_1 may not cause a significant change in α, or alternatively, it may cause S_1 to be rotated into an orientation where a new crenulation will not form (i.e. $\alpha > 30°$). Shear strain will be determined using p for the second-formed cleavage (p^*) and p' of the rotated first-formed cleavage and

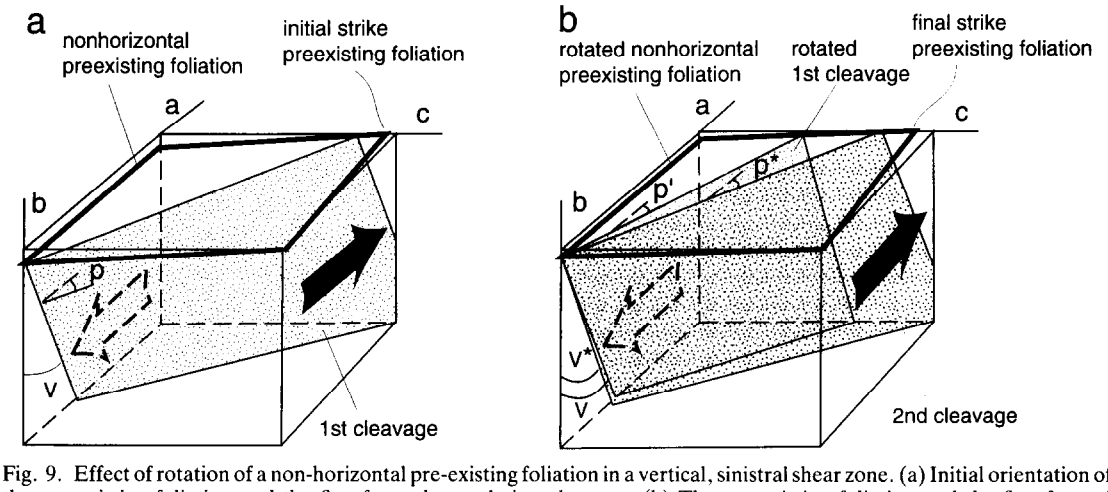

Fig. 9. Effect of rotation of a non-horizontal pre-existing foliation in a vertical, sinistral shear zone. (a) Initial orientation of the pre-existing foliation and the first-formed crenulation cleavage. (b) The pre-existing foliation and the first formed cleavage after rotation; shear strain: γ = 1. Position of the second cleavage that formed on the rotated pre-existing foliation is not equivalent to the initial orientation of the first-formed cleavage. Note the minor difference in v and p (for the first cleavage) and v^* and p^* (for the second cleavage). The second cleavage and rotated first cleavage intersection would lie slightly off the shear zone.

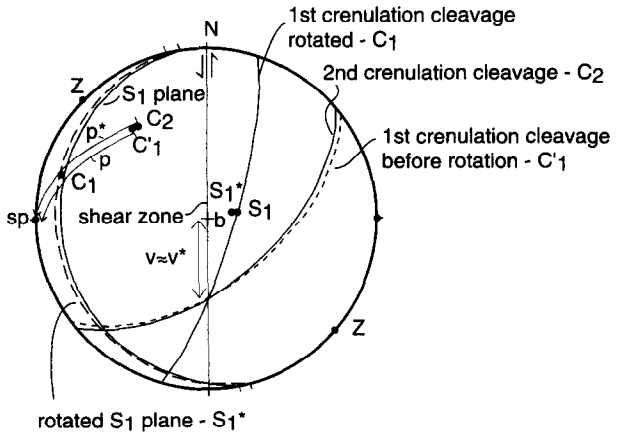

Fig. 10. Stereonet showing planes from Fig. 9. Note the minor differences in orientation of S_1 before and after rotation and of the first cleavage before rotation and the second cleavage. The intersections of these two with the rotated first cleavage are essentially the same.

the apparent v from the intersection of the two cleavages (Figs. 9 and 10). The amount of error in calculated shear strain depends on the difference between the initial orientation of the first-formed crenulation cleavage and the orientation of the second-formed cleavage. If no rotation of the pre-existing foliation occurs, these are the same.

To evaluate the effect of rotation of the pre-existing foliation, forward modeling using a shear zone with a known shortening direction was undertaken. In the models, the orientation in which a crenulation cleavage would form is determined for a given pre-existing foliation orientation. Then both the pre-existing foliation and crenulation cleavage are subjected to an increment of shear strain. After rotation of both, the orientation of a newly formed crenulation cleavage is determined (Figs. 9 and 10). The new crenulation cleavage and the rotated one are used to calculate the apparent shear zone orientation and the apparent shear strain. These apparent shear strains and the orientations of the apparent shear zones are then compared to the real values. The forward modeling shows that slightly oblique S_1 planes ($\leq 10°$ discordance from shear plane strikes and/or *ac* plane dips) show very little rotation, and the difference in orientation between the initial first-formed and second-formed crenulation cleavages is very small (Figs. 9 and 10). The difference in orientation is within field measurement error. Highly oblique planes, depending on their strikes and dips relative to that of the shear plane, either rotate into a position where a second crenulation will not form, or the crenulation cleavages have high v values ($>50°$). Moderately oblique planes undergo less rotation and generally have lower v values for the crenulation cleavages.

The effect of rotation of the pre-existing foliation is best evaluated using the magnitude of the initial v value of the first-formed crenulation. If the first-formed crenulation cleavage has a large initial v ($>50°$) and two crenulations form, either: (1) the v becomes smaller during subsequent shearing and the apparent shear strains are ± 1 of the real value; or (2) the calculated shear zones bisect the two crenulation cleavages and are at a moderately high angle to the real zones. In this case the shear strains cannot be calculated. For initial $v < 50°$, the effect is negligible, with shear strain errors usually much less than ± 1. The apparent shear zones are nearly parallel to the real zones with strikes off only a couple degrees and dips off up to a maximum of 20°. More specifically, for large shear strains and $v = 40°$ to 50°, errors are ± 1. For large shear strains and $v = 0$–40°, errors in γ are less than 0.5. For small shear strains, errors are about 0.2. Thus, for $v < 50°$, the calculated apparent shear strains should show very little error.

In summary, if the pre-existing foliation is parallel or nearly parallel to the *ac* plane, then its orientation will not affect the orientation in which the crenulations initiate. The amount of rotation of the pre-existing foliation is insignificant. For the cases in which the pre-existing foliation is at a small angle to the *ac* plane, the orientation of the pre-existing foliation affects the orientation at which the crenulation initiates. However, the error induced by ignoring any subsequent rotation of the pre-existing foliation is minor and decreases with decreasing shear strain. All of the cleavages used in the study area fall in one of these two cases. The example shown in Figs. 9 and 10 is typical of cases used in this study. Pre-existing foliations that are highly oblique to the *ac* plane greatly affect the orientation in which crenulations initiate and may undergo a significant amount of rotation along with the cleavages. For these cases where two cleavages form, either shear strains cannot be calculated or the error is still relatively minor. No cleavages formed on highly oblique planes were used in the study.

RESULTS

The above method of calculating incremental shear strains was attempted on 79 sets of superposed crenulation cleavages. Of these, 43 could be used to find reliable shear strains and these values are given in Table 1. Of those not included, most yielded calculated shear zones that bisected the crenulation cleavages, suggesting large initial v values for the first-formed crenulation cleavage and pre-existing foliations that were highly oblique to the *ac* plane (see previous section). Others that were not used either: (1) had low ϕ values and thus were outside the range tested by Gay & Weiss (1974); or (2) geometrically could not have formed as a result of progressive shearing unless the preexisting foliation was substantially rotated between formation of the two cleavages (i.e. synchronous large-scale folding). For all data, see Burks (1985).

For the majority (65%) of the crenulation cleavages that were usable, ϕ values are between 80 and 90°, p values are between 40° and 46° with most at 45° ± 1, and v values are between 0° and 2°. Thus, the pre-existing foliation was essentially parallel to the *ac* plane, and the shear strains show essentially no error. On a plot of $p - p'$ vs γ, these data define a curve essentially coincident

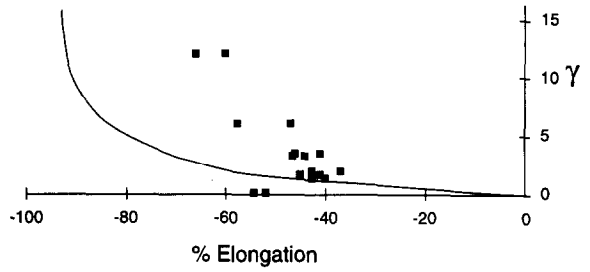

Fig. 11. Theoretical plot of % elongation vs shear strain (γ) with data for the crenulation cleavages. The % elongations for crenulation cleavages are approximate and represent minimum values. The values are calculated from eight crenulation sets in Table 2 using the highest and lowest buckling values and flattening strains.

with the $v = 0, p = 45$ theoretical curve (Fig. 7). For the rest, the foliations were inclined to the *ac* plane and the pre-existing foliation affected the orientation in which the crenulation cleavages formed. The ϕ values are between 42° and 79°, p between 20–36° and 63–88°, and v from 15° to 60°. These data show much more scatter on a plot of $p - p'$ vs γ (Fig. 7), as would be expected with the variable v and p values. When compared with the theoretical curves, the scatter in data can be seen to reflect different initial p and v values. Errors for these shear strains are very minor as $v < 50°$ for all but four. Of the four with $v > 50°$, none were over 60°. Thus the errors in these are still relatively small.

The range in shear strains is from 0 to 10 both for those where the pre-existing anisotropy had an effect on the orientation of the crenulation cleavages ($\phi < 80°$) and for those where it did not. The two anomalously high shear strains (18 and 51.6) occurred where p was small and shear strain values are sensitive to small rotations. Thus these two values are not considered valid. The primary difference between inclined and non-inclined pre-existing foliations relative to the *ac* plane is for the v values. All $v > 10°$ were for inclined foliations, and only one low v value (0°) was for an inclined foliation. The presence of v not equal to 0° need not indicate oblique-slip motion, but instead that the anisotropy of the pre-existing foliation affected the orientation in which the crenulation cleavages initiated. We cannot conclusively rule out oblique-slip motion for the inclined-foliation cases, but independent kinematic indicators and the superposed crenulation cleavages on non-inclined foliations indicate oblique-slip was minor.

The amount of shortening recorded by the crenulations was compared with that predicted from the calculated shear strains (Fig. 11) for eight samples for which both flattening and buckling strains were measured (Table 2). To estimate the total finite strain, all shortening recorded by a crenulation was assumed to occur instantaneously prior to rotation. Thus successive increments could be combined to find an approximate finite strain ellipsoid. For shear strains under 5, the amount of shortening is equal to or somewhat less than that predicted, indicating that only progressive simple shear is needed to account for the formation of these superposed crenulation cleavages. The slight difference may, in part, be attributed to the imprecise way the finite strains were estimated. Also, if the rotation of crenulation cleavages was not strictly passive, a possibility for the round-hinged crenulations, then some active hinge migration prior to locking without corresponding amplification could help explain the discrepancies. However, accommodation of the strain by other structures is also likely, especially for the large shear strains ($\gamma > 5$). In all samples, only the most penetrative and pervasive crenulation cleavages were used. Thus one possibility is that other, less pronounced crenulations are present that accommodated some of the shortening caused by the shearing. Layer parallel shortening prior to crenulation initiation or slight warping of the pre-existing foliation prior to initiation of large-scale folding could also explain the slight discrepancies. Nonetheless, as less shortening occurred than predicted for the measured shear strain, no additional component of coaxial strain is needed.

Comparison of D_3 (sinistral) and D_4 (dextral) superposed crenulations shows little difference in magnitude. The calculated incremental shear strain values for D_3 range from 0.2 to 7.8 and those for D_4 from 0.11 to 10.3 (with the two anomalous values removed); values of D_3 and D_4 shear strains for individual samples and shear zones are given on Fig. 1 and in Table 1. Localities with more than one value for either D_3 or D_4 contain more than two crenulation cleavages that formed during the same progressive deformation. Both D_3 and D_4 generally have N- to NE-trending shear planes, similar to those measured in the field. Sinistral cleavages show a greater variability in shear zone strike. This wider range in orientation occurs because sinistral zones have been reoriented by dextral zones and large-scale superposed folding accompanied sinistral shearing. If the widths of the individual shear zones were known, it would be possible to calculate the amount of displacement indicated by the shear strains determined using superposed crenulations. Unfortunately, as mentioned previously, the widths of most of these zones cannot be determined.

DISCUSSION

The results of using shear-related crenulation cleavages as strain markers within the Beaverhead shear zone have significance in terms of both examining strain mechanisms in ductile shear zones as well as in interpreting tectonic histories of the Narragansett Basin and southeastern New England. The superposed crenulation cleavages are valuable kinematic indicators in certain ductile shear zones, and their three-dimensional geometries are strain markers for quantifying minimum shear strains and finite displacements.

When applying this technique for quantifying incremental shear strains to other areas, it is important to determine that the cleavages formed as a result of progressive simple shear. If crenulations show a consistent overprinting relationship and are at small (<30°) angles to each other, such a mechanism for their formation is likely, especially if they are found in shear zones

or in the presence of other kinematic indicators. To check, their orientations and that of the pre-existing anisotropy and shear zone should be plotted on a stereonet to see if the geometry is appropriate for formation of the two or more cleavages by progressive deformation in the shear zone. When this information is plotted, it is a simple step to determine the p, p' and v values needed to calculate the shear strains. If the foliation is inclined to the *ac* plane, the effect of the pre-existing anisotropy on the initiation orientation of the crenulation cleavages and on the shear strains must be taken into consideration. If the orientation of the shear zone is unknown, it can be calculated using the methods outlined in this paper. In this case, there are a very few geometries of pre-existing foliation/shear plane that will not yield usable results. For these geometries, the formation of cleavages as a result of shearing cannot be confirmed or discounted. In general, the cleavages will be at angles of less than 30° to one another, unless the pre-existing foliation was highly oblique to the foliation resulting in large v values.

This technique to quantify incremental shear strains cannot be used in a general, non-coaxial strain field because it uses equations for progressive simple shear (Skjernaa 1980) to calculate shear strains and assumes that v does not change appreciably. In cases where the shear zone orientation must be calculated from the available data, this method also assumes that the incremental shortening direction (Z) is 45° to the shear plane, which need not be true for general, non-coaxial strain. Superposed crenulations can be used, however, as kinematic indicators in general, non-coaxial strain fields.

The contractional crenulation cleavages within the Narragansett Basin shear zones form after a minimum accumulation of layer-parallel, constant-volume strain is produced by progressive simple shear. Minor flattening across crenulation hinges, internal buckling along the pre-existing foliation, and internal rotation toward the local shear plane are the dominant deformation mechanisms involved in producing the crenulation morphology and geometry. The compatibility of the incremental shortening strains and that predicted by the shear strains indicates that no additional component of coaxial strain, such as that imparted by transpression, is needed to explain the deformation. The progressive simple shear of the metasedimentary rocks in the Narragansett Basin most likely results from strike-slip reactivation of underlying basement faults, as supported by the parallelism (and coincidence in some cases) of observed faults, shear zones and calculated shear planes.

The pre-existing anisotropy controls the direction of extension and shortening and therefore the orientation of the cleavages. If the pre-existing foliation is parallel or nearly parallel to the *ac* plane, the crenulation cleavage forms in the same orientation that a shear-related foliation would if the anisotropy was not present. If the pre-existing foliation is oblique to the *ac* plane but still at a high angle to the *b* direction, then its orientation affects that of the initiating crenulations. In addition, the subsequent rotation of this pre-existing anisotropy prior to the initiation of another crenulation generation introduces a slight error in the shear strain measurements. If the foliation becomes too oblique to the *ac* plane, crenulations may not form.

The crenulation cleavages are strain-sensitive and lose the ability to accommodate the shortening strain as they amplify and rotate toward the shear plane. When a crenulation starts to 'lock', it becomes easier to initiate another more favorably oriented crenulation. This new crenulation in turn undergoes the same process of rotation and amplification until it also 'locks' and a third one forms. Thus, each crenulation generation only records an increment of the shortening strain, and the angular relationship between superposed crenulation cleavages records the associated incremental shear strains. These strain-sensitive fabric elements rotate as material planes rather than as the XY plane of the finite strain ellipsoid. Therefore, the sets of superposed crenulation cleavages record the non-coaxial deformation path as well as the associated incremental shortening and shear strains.

CONCLUSIONS

Superposed crenulation cleavages are a strain-sensitive fabric that record incremental strains and the deformation path for well-foliated rocks in shear zones. In the Narragansett Basin, a nearly horizontal pre-existing foliation is deformed by vertical sinistral and dextral strike-slip zones. Because the pre-existing anisotropy is nearly parallel to the *ac* plane, crenulations form and rotate toward the shear plane. When the crenulations are no longer able to accommodate the incremental shortening strains, a new set forms at a small angle to the earlier set. With continued deformation, both sets of crenulations rotate toward the shear plane and another one may form. These sequentially formed crenulation cleavages track the deformation path and provide a new kinematic indicator for well-foliated rocks.

Acknowledgements—This paper represents part of the first author's Ph.D. dissertation and further research by the second author. Funding for the field portion of this study was provided through a National Science Foundation Grant (EAR-811-1294) to S. Mosher. Lodging while in the field was provided by Ft. Getty Recreation Area and the town of Jamestown, Rhode Island. Other support for the project was provided by the Geology Foundation of the Department of Geological Sciences, University of Texas at Austin. A. Goldstein, M. P. A. Jackson, C. Simpson, K. E. Carter and M. K. Johns are thanked for advice during the research; the present manuscript benefited from three anonymous reviews of an earlier version of this manuscript. D. R. Gray, A. J. Dennis and M. K. Johns are thanked for helpful reviews of the present manuscript.

REFERENCES

Berryhill, A. W. 1984. Structural analysis of progressive deformation within a complex strike-slip fault system: southern Narragansett Basin, Rhode Island. Unpublished M.A. thesis, University of Texas at Austin.

Berthe, D., Choukroune, P. & Jegouzo, P. 1979. Orthogneiss, mylon-

ite and non-coaxial deformation of granites: the example of the South American Shear-Zone. *J. Struct. Geol.* **1**, 31–42.
Borradaile, G. J., Bayly, M. B. & Powell, C. McA. 1982. *Atlas of Deformational and Metamorphic Rock Fabrics*. Springer, Berlin.
Boulter, C. A. & Raheim, A. 1974. Variations in Si^{4+} content of phengites through a three stage deformation sequence. *Contr. Mineral. Petrol.* **48**, 57–71.
Burks, R. J. 1984. Finite and incremental strains along ductile shear zones, Narragansett Basin, RI. (Abstract.) *Geol. Soc. Am. Ab. w. Prog.* **16**, 459.
Burks, R. J. 1985. Incremental and finite strain analyses within ductile shear zones, Narragansett Basin, Rhode Island. Unpublished Ph.D. thesis, University of Texas at Austin.
Cobbold, P. R. & Watkinson, A. J. 1981. Bending anisotropy: a mechanical constraint on the orientation of fold axes in an anisotropic medium. *Tectonophysics* **72**, T1–T10.
Cogswell, J. P. Mahler & Mosher, S. 1994. Late-stage Alleghanian wrenching of the southwestern Narragansett Basin, Rhode Island. *Am. J. Sci.* **294**, 861–901.
Dennis, A. J. & Secor, D. T. 1987. A model for the development of crenulations in shear zones with applications from the southern Appalachian Piedmont. *J. Struct. Geol.* **9**, 809–817.
Donath, F. A. 1968. Experimental study of kinkband development in Martinsburg slate. In: *Research in Tectonics* (edited by Baer, A. J. & Norris, D. K.). *Geol. Surv. Pap. Can.* **68–52**, 255–288.
Durney, D. W. & Ramsay, J. G. 1973. Incremental strains measured by systematic crystal growths. In: *Gravity and Tectonics* (edited by DeJong, K. A. & Scholten, R.). Wiley and Sons, New York, 67–96.
Flinn, D. 1962. On folding during three dimensional progressive deformation. *Q. J. geol. Soc. Lond.* **118**, 385–433.
Gay, N. C. & Weiss, L. E. 1974. The relationship between principal stress directions and the geometry of kinks in foliated rocks. *Tectonophysics* **21**, 287–300.
Ghosh, S. K. & Ramberg, H. 1968. Buckling experiments on intersecting fold patterns. *Tectonophysics* **5**, 89–105.
Gray, D. R. 1977. Some parameters which affect the morphology of crenulation cleavages. *J. Geol.* **85**, 763–780.
Gray, D. R. & Durney, D. W. 1979. Investigations on the mechanical significance of crenulation cleavage. *Tectonophysics* **58**, 35–79.
Henderson, C. M. & Mosher, S. 1983. Narragansett Basin, Rhode Island: role of intrabasinal horsts and grabens in Alleghanian deformation. (Abstract.) *Geol. Soc. Am. Ab. w. Prog.* **15**, 129.
Hudleston, P. J. 1973. Fold morphology and some geometrical implications of theories of fold development. *Tectonophysics* **16**, 1–46.
Ingles, J. 1985. Theoretical and natural strain patterns in ductile simple shear zones. *Tectonophysics* **115**, 315–334.
Lister, G. S. & Snoke, A. W. 1984. *S–C* mylonites. *J. Struct. Geol.* **6**, 617–638.
Mosher, S. 1983. Kinematic history of the Narragansett Basin, Massachusetts and Rhode Island: constraints on late Paleozoic plate reconstructions. *Tectonics* **2**, 327–344.
Mosher, S. & Berryhill, A. W. 1991. Structural analysis of progressive deformation within complex transcurrent shear zone systems: southern Narragansett Basin, Rhode Island. *J. Struct. Geol.* **13**, 557–578.
Mukhopadhyay, D., Sengupta, S. & Bhattacharya, S. 1969. Strain measurements in some Precambrian rocks of eastern India and their bearing on the tectonic significance of schistosity. *J. Geol.* **77**, 703–710.
Odonne, F. & Vialon, P. 1987. Hinge migration as a mechanism of superimposed folding. *J. Struct. Geol.* **9**, 835–844.
Platt, J. P. 1979. Extensional crenulation cleavage. *J. Struct. Geol.* **1**, 95.
Platt, J. P. & Vissers, R. L. M. 1980. Extensional structures in anisotropic rocks. *J. Struct. Geol.* **2**, 397–410.
Ramsay, J. G. 1967. *Folding and Fracturing of Rocks*. McGraw-Hill, New York.
Ramsay, J. G. & Huber, M. I. 1983. *The Techniques of Modern Structural Geology: Volume* 1: *Strain Analysis*. Academic Press, New York.
Ramsay, J. G. & Huber, M. I. 1986. *The Techniques of Modern Structural Geology: Volume* 2: *Folds and Fractures*. Academic Press, New York.
Ridley, J. 1986. Parallel stretching lineations and fold axes oblique to a shear displacement direction—a model and observations. *J. Struct. Geol.* **8**, 647–653.
Skehan, J. W. & Murray, D. P. 1979. A geologic profile across southeastern New England. *Tectonophysics* **69**, 285–319.
Skjernaa, L. 1980. Rotation and deformation of randomly oriented planar and linear structures in progressive simple shear. *J. Struct. Geol.* **2**, 101–109.
Snoke, A. W. & Mosher, S. 1989. The Alleghanian orogeny as manifested in the Appalachian internides. In: *The Appalachian–Ouchita Orogen in the United States* (edited by Hatcher, R. D., Veile, G. W. & Thomas, W. A.). *Geol. Soc. Am.* **F-2**, 288–318.
Treagus, J. E. & Treagus, S. H. 1981. Folds and the strain ellipsoid: a general model. *J. Struct. Geol.* **3**, 1–17.
Watkinson, A. J. 1983. Patterns of folding and strain influenced by linearly anisotropic bands. *J. Struct. Geol.* **5**, 449–454.
Watkinson, A. J. & Cobbold, P. R. 1981. Axial directions of folds in rocks with linear/planar fabrics. *J. Struct. Geol.* **3**, 211–217.
Wickham, J. S. 1973. An estimate of strain increments in a naturally deformed carbonate rock. *Am. J. Sci.* **273**, 23–47.
Williams, P. F. & Price, G. P. 1990. Origin of kink-bands and shear-band cleavage in shear zones: an experimental study. *J. Struct. Geol.* **12**, 145–164.